Power allocation for uniform illumination with stochastic LED arrays

G. V. S. S. Praneeth Varma,[1,*] Rayapati Sushma,[1] Vandana Sharma,[2] Abhinav Kumar,[1] and G. V. V. Sharma[1]

[1]*Department of Electrical Engineering, Indian Institute of Technology Hyderabad, Telangana, 502285, India*

[2]*Department of Physics, Indian Institute of Technology Hyderabad, Telangana, 502285, India*

[*]*ee14resch11007@iith.ac.in*

Abstract: In this paper, a simple heuristic power allocation scheme is proposed for a random LED array to obtain uniform irradiance on the projection surface. This is done by considering a binomial point process (BPP) for modeling the LED location and using the quality factor as a performance metric. Numerical results are provided to validate the proposed model and demonstrate its simplicity over existing LED geometries.

References and links

1. H. Guo-yong, C. Chang-ying, and C. Zhen-qiang, "Free-space optical communication using visible light," J. Zhejiang Univ. Sci. A **8**(2), 186–191 (2007).
2. J. Kovác, J. Jakabovic, and M. Kytka, "Advanced light emitting devices for optoelectronic applications," Proc. SPIE **7138**, 71382A (2008).
3. J. Kahn and J. Barry, "Wireless infrared communications," Proc. IEEE **85**(2), 265–298 (1997).
4. T. Komine and M. Nakagawa, "Fundamental analysis for visible-light communication system using led lights," IEEE Trans. Consum. Electron. **50**(1), 100–107 (2004).
5. I. Moreno, "Configuration of led arrays for uniform illumination," Proc. SPIE **5622**, 713–718 (2004).
6. I. Moreno, "Design of led spherical lamps for uniform far-field illumination," Proc. SPIE **6046**, 60462E (2006).
7. N. Wittels and M. A. Gennert, "Optimal lighting design to maximize illumination uniformity," Proc. SPIE **2348**, 46 (1994).
8. M. A. Gennert, N. Wittels, and G. L. Leatherman, "Uniform frontal illumination of planar surfaces: where to place the lamps," Opt. Eng. **32**(6), 1261–1271 (2005).
9. I. Moreno, M. Avendaño-Alejo, and R. I. Tzonchev, "Designing light-emitting diode arrays for uniform near-field irradiance," Appl. Opt. **45**(10), 2265–2272 (2006).
10. Z. Qin, K. Wang, F. Chen, X. Luo, and S. Liu, "Analysis of condition for uniform lighting generated by array of light emitting diodes with large view angle," Opt. Express **18**(16), 17460–17476 (2010).
11. A. J. W. Whang, Y. Y. Chen, and Y. T. Teng, "Designing uniform illumination systems by surface-tailored lens and configurations of LED arrays," J. Display Technol. **5**(3), 94–103 (2009).
12. K. Wang, D. Wu, Z. Qin, F. Chen, X. Luo, and S. Liu, "New reversing design method for LED uniform illumination," Opt. Express **19**(S4), A830–A840 (2011).
13. Y. Tanaka, T. Komine, S. Haruyama, and M. Nakagawa,"Indoor visible light transmission system utilizing white LED lights," IEICE Trans. Commun. **E86-B**(8), 2440–2454 (2003).
14. Y. Tanaka, S. Haruyama, and M. Nakagawa, "Wireless optical transmission with the white colored LED for the wireless home link," in *Int. Symposium on Personal, Indoor and Mobile Radio Communications* (2000), pp. 1325–1329.
15. T. Komine, Y. Tanaka, S. Haruyama, and M. Nakagawa, "Basic study on visible-light communication using light emitting diode illumination," in *International Symposium on Microwave and Optical Technology* (2001), pp 45-48.
16. H.-C. Chen, C.-J. Liou, and S.-R. Siao,"Illumination distribution and signal transmission for indoor visible light communication with different light-emitting diode arrays and pre-equality circuits," Opt. Eng. **54**(11), 115106 (2015).
17. T. Komine and M. Nakagawa, "Integrated system of white LED visible-light communication and power-line communication," IEEE Trans. Consum. Electron. **49**(1), 71–79 (2003).
18. Z. Wang, C. Yu, W.-D. Zhong, J. Chen, and W. Chen, "Performance of a novel LED lamp arrangement to reduce SNR fluctuation for multi-user visible light communication systems," Opt. Express **20**(4), 4564–4573 (2012).
19. J. Ding, Z. Huang, and Y. Ji, "Evolutionary algorithm based power coverage optimization for visible light communications," IEEE Commun. Lett. **16**(4), 439–441 (2012).

20. Y. Liu, Y. Peng, Y. Liu, and K. Long, "Optimization of receiving power distribution using genetic algorithm for visible light communication," Proc. SPIE **9679**, 96790I (2015).
21. H. Zheng, J. Chen, C. Yu, and M. Gurusamy, "Inverse design of led arrangement for visible light communication systems," Opt. Commun. **382**, 615–623 (2017).
22. S. Pal, "Optimization of LED array for uniform illumination over a target plane by evolutionary programming," Appl. Opt. **54**(27), 8221–8227 (2015).
23. P. Lei, Q. Wang, and H. Zou,"Designing LED array for uniform illumination based on local search algorithm," J. Europ. Opt. Soc. Rap. Publ. **9**, 14014 (2014).
24. S. Srinivasa and M. Haenggi, "Distance distributions in finite uniformly random networks: theory and applications," IEEE Trans. Veh. Technol. **59**(2), 940–949 (2010).
25. Y. Chen, C. W. Sung, S.-W. Ho, and W. S. Wong, "Ber analysis for interfering visible light communication systems," in *International Symposium on Communication Systems, Networks and Digital Signal Processing* (2016), pp. 564–570.
26. W. H. Press, S. A. Teukolsky, W. T. Vetterling, and B. P. Flannery, '*Numerical Recipes: The Art of Scientific Computing* (Cambridge University Press, 2007).

1. Introduction

Light has traditionally been used for making objects visible to the naked eye. Lately, there has been tremendous interest in using it for free space communication [1]. This has simultaneously been accompanied by significant interest in light emitting diodes (LEDs) that have been replacing conventional light sources in almost all applications [2–4]. LEDs are better than existing incandescent lamps in terms of long life expectancy, high tolerance to humidity, low power consumption, and minimal heat generation. Fair amount of existing literature has focused on achieving uniform irradiance over a planar surface [5–8], beginning with the problem of finding the optimal LED geometry at the light source to achieve uniform irradiance [9]. This was done by using the irradiance distributions at the closest points on the incident surface. The case of LEDs using a freeform lens with a large view angle has been considered in [10]. More literature on similar themes is available in [11, 12]. In [13], the properties of white LEDs were studied and shown to be useful for indoor optical transmission. More literature on using white LEDs for communication is available in [14–17].

Some of the above literature has focused on a regular geometry with equal power allocation to individual LED sources. While uniform illuminance is desirable, optimal power consumption is an extremely important factor in the design of LED light sources. To address this, recent literature has focused on power allocation, along with flexility in the LED source geometry to achieve uniform irradiance [18–21].

Several power allocation schemes have been proposed to achieve uniform irradiance for visible light communication (VLC) applications [18–21]. A trial and error approach for power allocation for uniform irradiance is used in [18] for a combination of circular square geometry in order to illuminate the edges of the incident surface. An evolutionary algorithm based optimization scheme is proposed in [19] to modify the power of LED transmitters to reduce the signal power fluctuation at the receiver. In [20], a genetic algorithm is proposed to optimize the refractive indices of the concentrators on receivers to achieve a uniform distribution of the received power. An optimal LED arrangement to achieve uniform irradiance is investigated as a convex optimization problem in [21]. The optimization of the location of an irregular LED array for uniform irradiance is discussed in [22, 23].

In all the above, computationally intensive optimization routines were used for power allocation for the LED sources to realise uniform irradiance on the incident surface. The system proposed in [21] departs from the conventional model by considering arbitrary locations for the LED sources. The most practical scenario would be the case when the LEDs are placed randomly at the source with uniform illumination being achieved through power allocation, keeping the total power constant. This problem is addressed in this paper by considering a binomial point process (BPP) based stochastic geometry [24]. Further, a simple metaheuristic

power allocation scheme is proposed for uniform irradiance on the incident surface. Power allocation is done by maximizing a metric for uniformity of the signal to noise ratio (SNR) at the output of the photodetector. Through numerical results, it is shown that the performance of the BPP model and the associated power allocation is comparable to the model in [18].

Table 1. System Model Parameters

Symbol	Description
N	Number of source LEDs
$P = \sum_{i=1}^{N} P_{t_i}$	Total power allocated to the source
P_{t_i}	Transmit power at ith node
P_{r_j}	Received power at jth photodetector
h	Distance between the transmit and receive surfaces
σ_j^2	Noise variance at the jth photodetector
$H_{ij} = \frac{(m+1) A \cos^m(\phi) \cos(\psi)}{2\pi d_{ij}^2}$	Propagation loss with distance
$m = \frac{\ln\left(\frac{1}{2}\right)}{\ln\left(\cos\left(\phi_{\frac{1}{2}}\right)\right)}$	Order of Lambertian emission
R	Responsivity
$\phi_{\frac{1}{2}}$	LED semi-angle at half power
d_{ij}	Distance between ith LED and jth photodetector
$\phi = \cos^{-1} \frac{h}{d}$	Angle of incident light
θ	Inclination of the photodetector to the incident surface

2. Preliminaries

Using the Lambertian radiation pattern to model the LED radiant intensity [3, 4],

$$R(\phi) = \frac{(m+1)\cos^m(\phi)}{2\pi},$$

(1)

where ϕ is the angle of incidence of light on the surface and m is the order of Lambertian emission, with $\phi_{\frac{1}{2}}$ being the LED semi-angle at half power, provided by the manufacturer. The channel direct current (DC) gain can then be expressed as [3, 4]

$$H = \frac{R(\phi)\cos(\theta)A}{d^2} = \frac{(m+1)\cos^m(\phi) A \cos(\theta)}{2\pi d^2}$$

(2)

where d is the distance between the LED and the photo-detector, A is the physical area of photodetector, and θ is the inclination of the photodetector to the incident surface. All system parameters are defined in Table 1.

3. System model

Consider the random source geometry generated using a BPP for $N = 16$ LEDs as shown in Fig. 1. The photo-detectors lie in a plane parallel to the LED array plane. The electrical signal
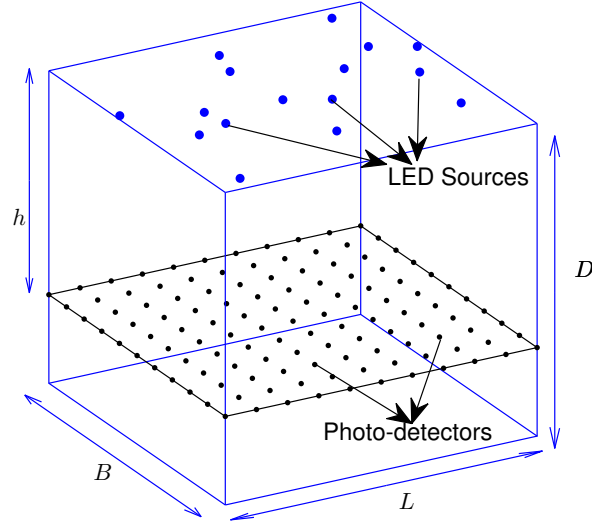
Fig. 1. System model.

at the output of the photodetector can be expressed as (see Table 1 for description of various parameters)

$$y_j = RP_{r_j} + n_j, \tag{3}$$

where the received optical power at the photodetector j

$$P_{r_j} = \sum_{i=1}^{N} H_{ij} P_{t_i}, \tag{4}$$

and H_{ij} is obtained from Eq. (2) and Table 1 as

$$H_{ij} = \frac{(m+1) Ah^{m+1}}{2\pi d_{ij}^{m+3}} \tag{5}$$

by assuming $\theta = \phi$ and substituting $\cos(\phi) = \frac{h}{d}$. d_{ij} is the distance between LED i and photo-detector j. n_j in Eq. (3) is additive white Gaussian noise (AWGN) with $n_j \sim \mathcal{N}\left(0, \sigma_j^2\right)$.

3.1. BPP

In a BPP stochastic array, N LEDs are placed randomly within a square of length l at the points $(x_n, y_n) : x_n, y_n \sim U(-l/2, l/2), \forall n = \{1 \cdots N\}$, according to a uniform distribution U defined by

$$p_U(u) = \begin{cases} \frac{1}{l} & -\frac{l}{2} \le u \le \frac{l}{2} \\ 0 & \text{otherwise} \end{cases} \tag{6}$$

where U is a random variable distributed uniformly between $\left(-\frac{l}{2}, \frac{l}{2}\right)$ and p_U is the corresponding probability density function (PDF).

3.2. Noise at the photodetector

The noise at the photodetector is the sum of the contributions from shot noise and thermal noise, and expressed as [25]

$$\sigma_j^2 = \sigma_{shot}^2 + \sigma_{thermal}^2, \tag{7}$$

where

$$\sigma_{shot}^2 = 2qRP_{r_j}B_N + 2qI_{bg}I_2B_N,$$

$$\sigma_{thermal}^2 = \frac{8\pi kT_k}{G}\eta AI_2B_N^2 + \frac{16\pi^2 kT_k\Gamma}{g_m}\eta^2 A^2 I_3 B_N^3 \tag{8}$$

with the parameters defined in Table 2.

Table 2. Sample Noise Parameters

Parameters	Symbol	Configuration
Boltzmann constant	k	$1.38064852 \times 10^{-23}m^2kgs^{-2}K^{-1}$
Electronic charge	q	$1.60217662 \times 10^{-19}C$
Area of Photodetector	A	$10^{-4}m^2$
Fixed capacitance of photodetector	η	$112pF/cm^2$
Responsivity	R	$1A/W$
Noise bandwidth	B_N	$100MHz$
Background current	I_{bg}	$5100\mu A$
Noise bandwidth factors	I_2, I_3	$0.562, 0.0868$
Absolute temperature	T_k	$295K$
Open-loop voltage gain	G	10
FET channel noise factor	Γ	1.5
FET transconductance	g_m	$30mS$

3.3. Quality factor

The quality factor, defined in [18] for measuring the irradiance performance of the light source, can be expressed as

$$F_\Lambda = \frac{\overline{\Lambda}}{2\sqrt{\text{var}(\Lambda)}}, \tag{9}$$

where

$$\Lambda_j = \frac{P_{r_j}}{\sigma_j^2} \tag{10}$$

is the received signal to noise ratio (SNR) at the jth photodetector and $\overline{\Lambda}$ and $\text{var}(\Lambda)$ are the mean and variance of $\left\{\Lambda_j\right\}_{j=1}^K$, where K is the number of photodetectors. For uniform illumination, it is important that the mean $\overline{\Lambda}$ be large and the variance $\text{var}(\Lambda)$ be small, resulting

in Eq. (9). Since the output of the photodetector is an electrical signal which is affected by noise, it is important to consider the SNR Λ_j while computing the quality factor in Eq. (9).

4. Motivation

Consider the various source geometries for $N = 16$ LEDs in Fig. 2. Using Eq. (10), the respective SNR profiles for the sources in Fig. 2(a) and 2(b) are plotted in Fig. 3, when each of the LEDs has equal power. Circular geometries are limited by their inability to sufficiently illuminate the corners of the incident surface. Figure 4(a) has the SNR profile for the source

(a) Circular geometry.

(b) Concentric circular geometry.

(c) A realization of BPP.

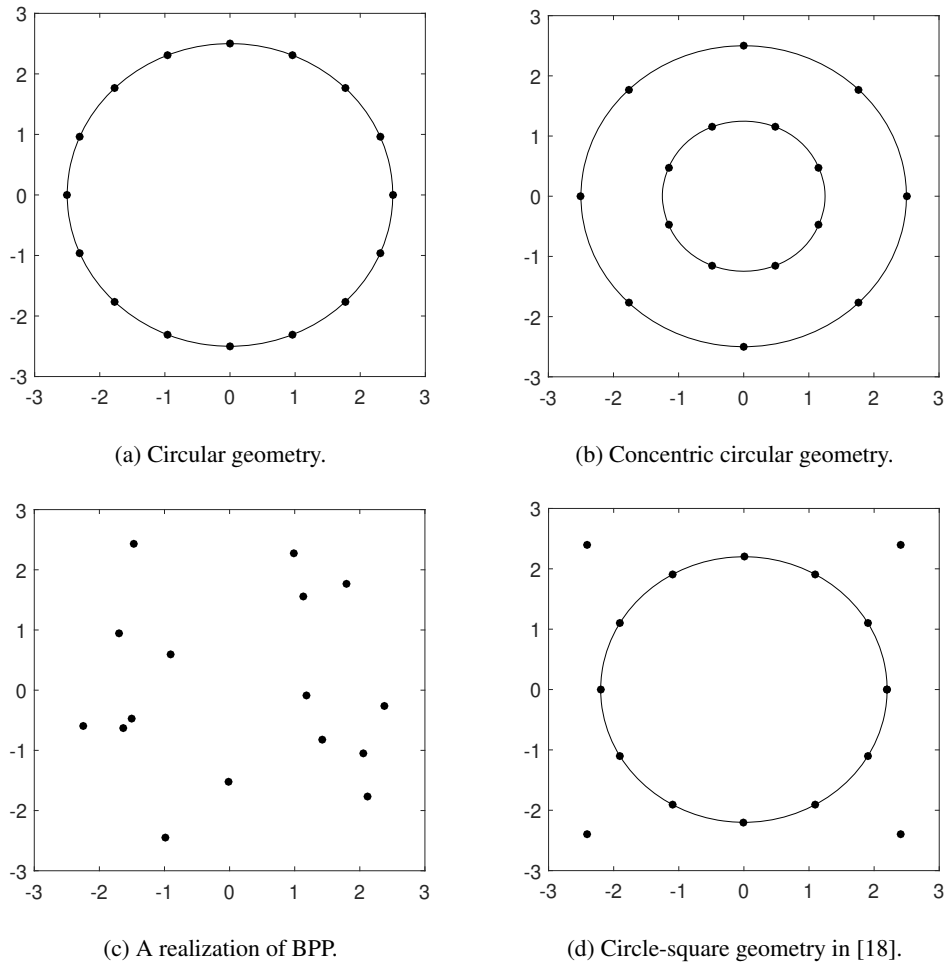(d) Circle-square geometry in [18].

Fig. 2. Arrangement of LEDs for different geometries.

in Fig. 2(d), with optimal locations for the LEDs on the circle as well as the corners [18] with equal power. Due to this optimal location, the arrangement in Fig. 2(d) has a more uniform SNR profile, since the coverage at the edges is better. The performance improves with optimal power allocation, as shown in Fig. 4(b).

Figure 4 and [18] indicate that LED sources distributed over an area according to a fixed geometry can achieve uniform irradiance with optimal location and power. In practice, LED sources used for illuminating larger areas may not follow a fixed geometry. When the locations of the LED sources are fixed but do not follow a definite pattern, like in Fig. 2(c), the geometry
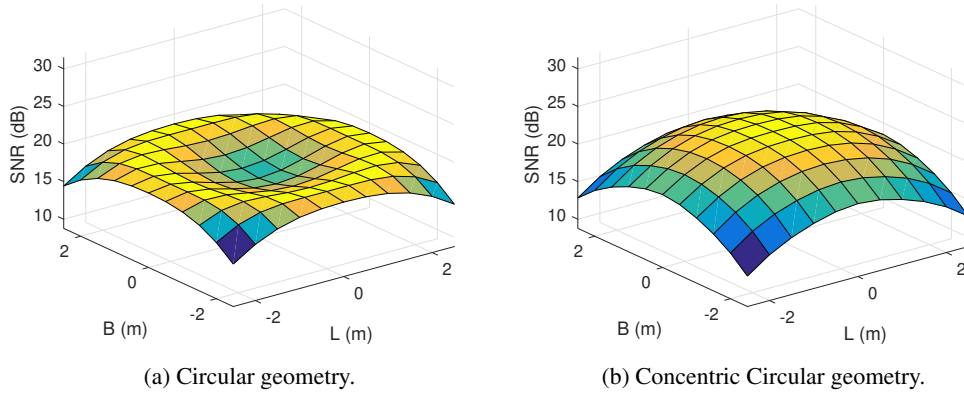
(a) Circular geometry.

(b) Concentric Circular geometry.

Fig. 3. SNR distribution with equal power allocation.

(a) With equal power allocation and optimal location.

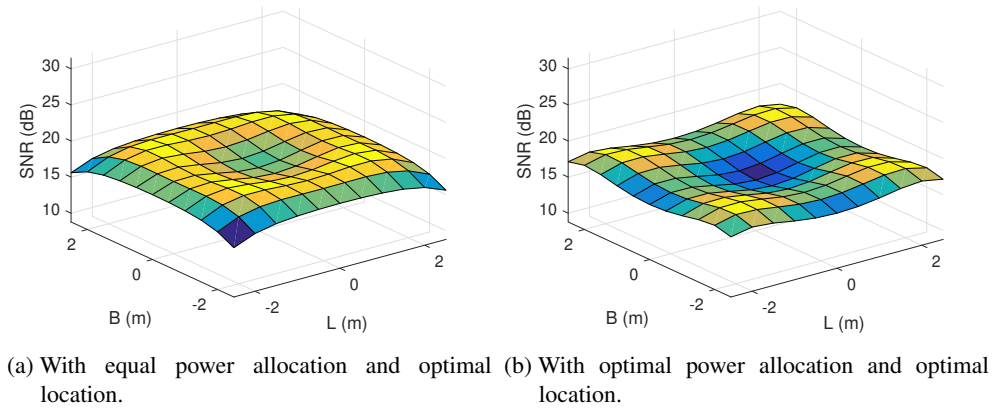(b) With optimal power allocation and optimal location.

Fig. 4. SNR distribution for circle-square geometry.

can be modeled using a BPP. In such cases, one possible way to obtain uniform illumination is through optimal power allocation by using the statistics of the BPP.

5. Power allocation for a BPP array

For a BPP, each LED is at a random location, so, heuristically, the power should also depend on the distance of the LED from the center of the array. The proposed power allocation is

$$P_{t_i} = \frac{r_i^\alpha}{\sum_{i=1}^N r_i^\alpha} P, \tag{11}$$

where P is the total source power, r_i is the location of the ith LED from the centre, α is a suitable exponent and P_{t_i} is the power allocated to the ith LED. The heuristic in Eq. (11) makes the power allocation suboptimal. For a BPP,

$$\Lambda_j = \mathbb{E}_\Phi \left[\frac{P_{r_j}}{\sigma_j^2} \right] \tag{12}$$

where $\mathbb{E}_\Phi$ is the expectation with respect to the BPP. Plotting the quality factor $F_\Lambda(\alpha)$ in Eq. (9) with respect to α in Fig. 5, $F_\Lambda(\alpha)$ appears to be concave and has a maximum. An optimal value

of α can then be obtained as
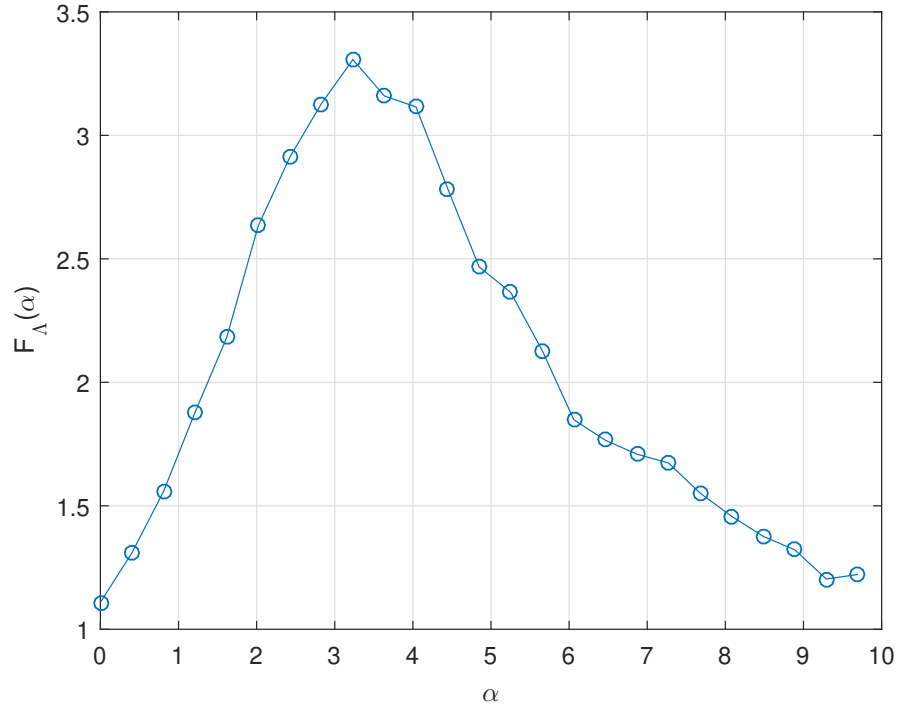
$$\max_{\alpha} F_{\Lambda}(\alpha), \tag{13}$$

Fig. 5. $F_{\Lambda}(\alpha)$ has a maximum.

5.1. Algorithm for optimal α

The golden section search algorithm [26] in Fig. 6 is used for finding the optimum value of α in Eq. (11)

Table 3. Simulation Parameters

Parameters	Symbol	Configuration
Room size	$L \times B \times D$	$5m \times 5m \times 3m$
Hieght of receiver plane	h_r	$0.85m$
Modulation index	M_I	1
LED semiangle	$\phi_{\frac{1}{2}}$	60°

6. Results

The simulation parameters for the results obtained in this section are available in Tables 2 and 3 and are similar to those used in [18] and [25]. A simple search routine for maximizing $F_{\Lambda}(\alpha)$ in Eq. (9) using Fig. 5 results in $\alpha \approx 3.1$. The value remains unchanged for higher values of
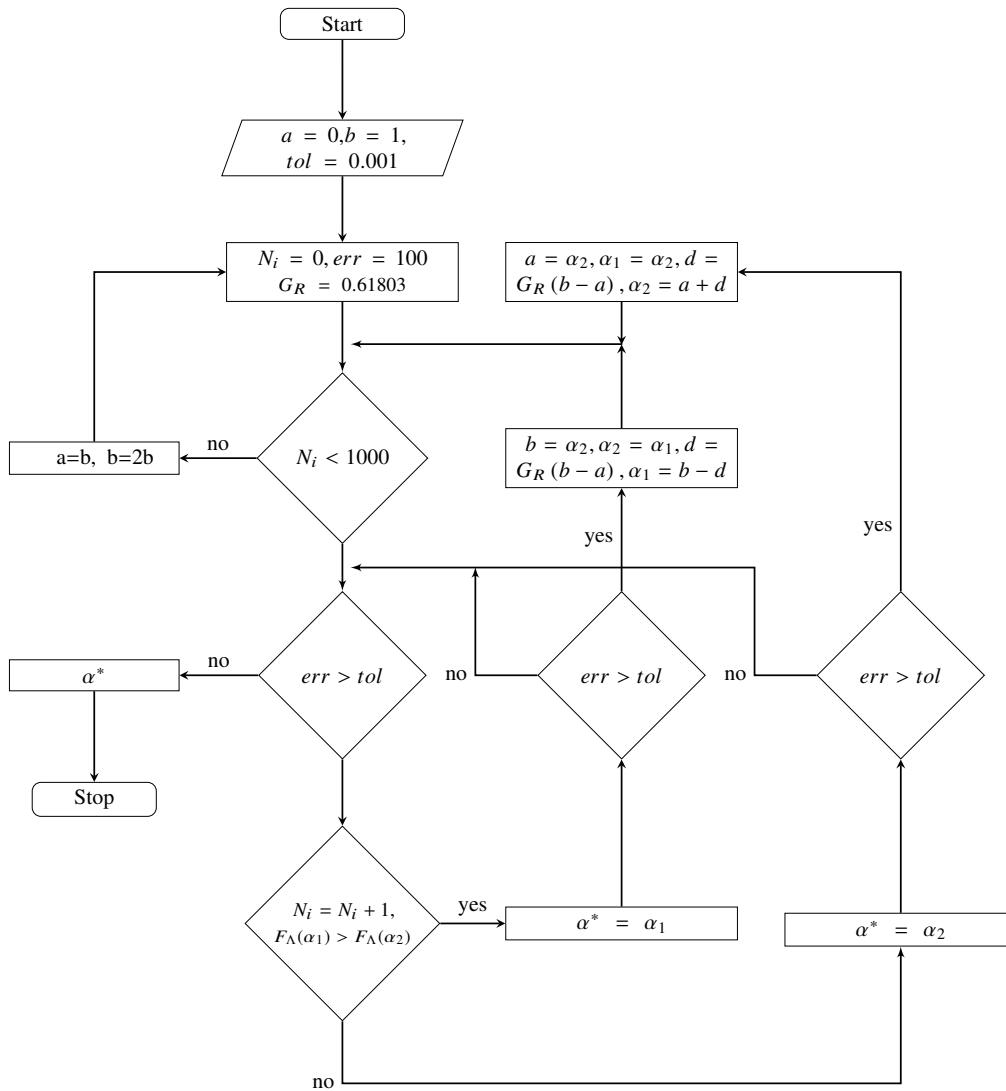
Fig. 6. Golden section search algorithm.

N. This value is used in Eq. (12) and Eq. (11) to calculate the SNR profile. Figure 7 shows the SNR profiles calculated using Eq. (12) with and without power allocation for the BPP in Fig. 2(c). The SNR profile for $N = 64$ for two different BPP realizations with suboptimal power allocation is provided in Fig. 8. From Fig. 8, it is obvious that the heuristic power allocation scheme in Eq. (11) results in a uniform SNR profile. Also, the F_Λ value in Table 4 for the BPP in Fig. 2(c) is close to that of the circle-square array in Fig. 2(d), indicating that the BPP with even suboptimal power allocation performs as well as a fixed geometry with optimal power allocation.

7. Conclusion

In this paper, it was shown that distributed LED sources that do not follow a locational pattern can be modeled using a BPP with appropriate power allocation, to achieve uniform illumination.
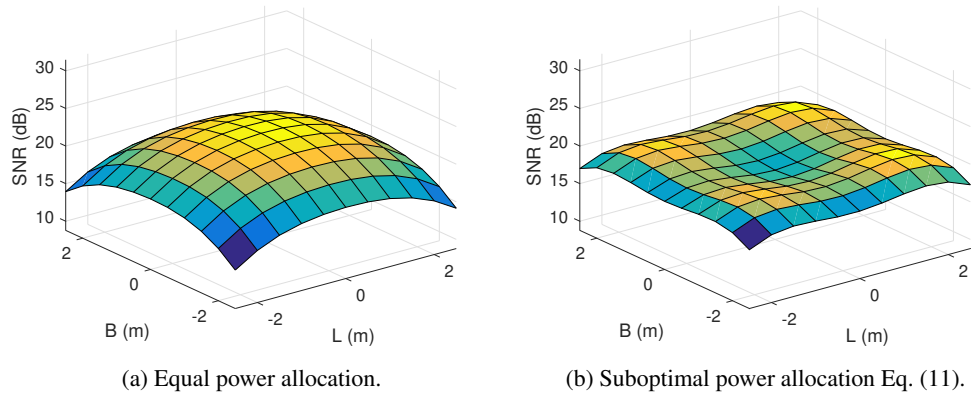
(a) Equal power allocation.

(b) Suboptimal power allocation Eq. (11).

Fig. 7. Average SNR for a BPP. $N = 16$.

(a) $N = 64$, BPP realization 1.

(b) $N = 64$, BPP realization 2.

(c) SNR profile for realization 1.

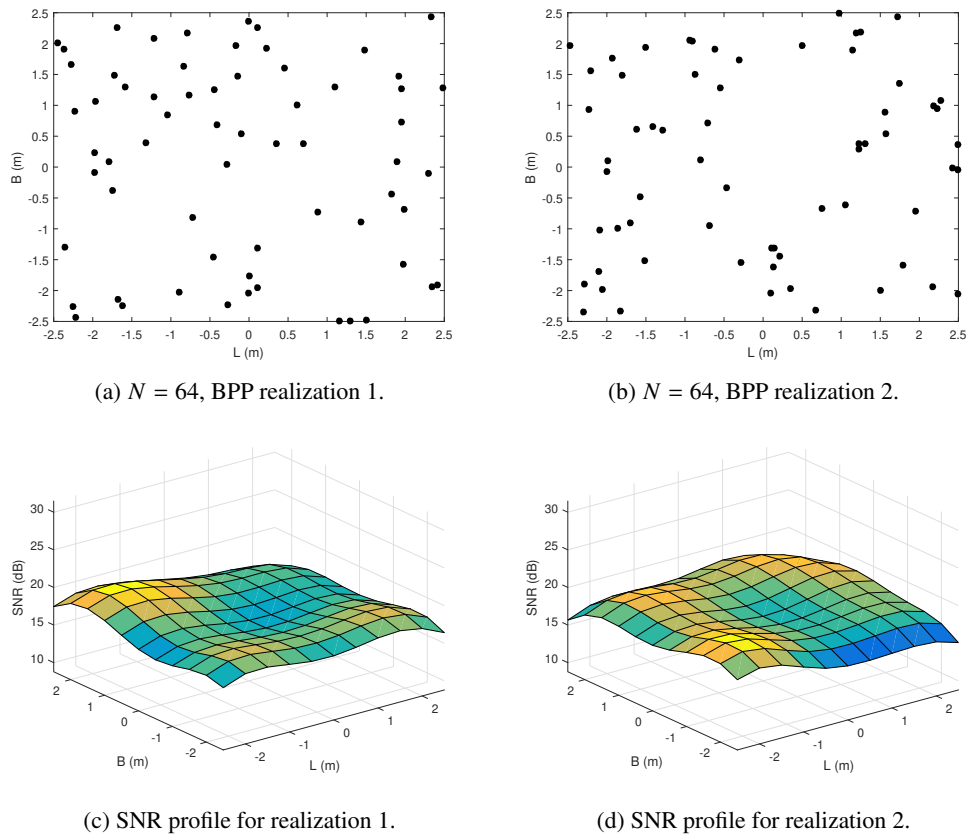(d) SNR profile for realization 2.

Fig. 8. SNR for two different realizations for $N = 64$. Uniform irradiance possible with different realizations.

This makes it extremely useful in practical applications like visible light communication where the source geometry is likely to be random. Though suboptimal, the proposed heuristic for power allocation is much simpler, resulting in reduced computational cost, when compared

Table 4. SNR Performance

	Circle-square		BPP	
	Equal Power	Optimal Power	Equal Power	Proposed heuristic
$\overline{\Lambda}$ (dB)	18.2658	17.3447	20.1121	18.8510
var (Λ) (dB)	21.4585	17.8065	33.5970	21.1082
F_{Λ}	2.8355	3.4924	1.0723	3.3780

to existing optimal power allocation schemes. Finding a simple but optimal power allocation scheme for stochastic LED arrays will be the focus of future work.